Bicycle and Motorcycle Dynamics 2019
Symposium on the Dynamics and Control of Single Track Vehicles,
9 – 11 September 2019, University of Padova, Italy

Practical Realization of a Theoretical Optimal-Handling Bicycle

Roy Gilboa, Anastasia Kubicki, Anthony Toribio, Mont Hubbard, and Jason K. Moore

Department of Mechanical and Aerospace Engineering
University of California, Davis
Davis, CA, USA
e-mail: rgilboa@ucdavis.edu, amkubicki@ucdavis.edu, artoribio@ucdavis.edu,,
mhubbard@ucdavis.edu, jkm@ucdavis.edu

ABSTRACT

Although conventional bicycles have evolved into the familiar fundamental design, there may exist bicycle designs that handle better when performing lateral maneuvers. Prior studies have provided evidence that optimizing for handling by varying trail, wheelbase, steer axis tilt, front wheel radius, and front wheel inertia can produce such bicycle designs. The present research goal is to practically realize and fabricate one of these theoretically optimal bicycle designs and evaluate whether it does in fact have better lateral handling qualities than a traditional bicycle. To this end, a theoretically optimal bike design was designed and fabricated based on the parameters of a track bicycle. The bicycle exhibits exceptional handling in simulation and the fabricated bicycle is rideable. Future work will subjectively and objectively evaluate the handling of the bicycle.

Keywords: bicycle, design, handling qualities, control, optimization, fabrication

1 INTRODUCTION

Our measure of lateral handling difficulty is the theoretical handling quality metric (HQM) presented in [1]. This HQM is a function of frequency and quantifies the human control effort needed to stabilize and direct a given bicycle based on quantifying the rider's roll rate sensing activity. Smaller peak values of HQM correspond to better lateral handling. HQM can be predicted for any given set of bicycle design parameters and specific travel speeds that yield a closed loop stable bicycle. HQM varies largely with speed, as well as different configurations of bicycle physical parameters: geometry, mass, and moments of inertia. We currently only consider the effects modeled by the Whipple-Carvallo model [2] even though there are other important physical inputs, e.g. tire force generation.

Two important conclusions arise from [1] and [3]. First, differences in handling due to physical parameter variations are more prominent at low speeds (less than 5 m/s for typical bicycles). Second, unique combinations of physical parameters can lower the HQM significantly. In [3], Moore, Hubbard, and Hess present an optimization method to arrive at theoretically optimal bicycle designs. We make use of a slightly modified version of that method to arrive at a target physically realizable design that has an optimally minimal peak HQM. We then followed an iterative design process to develop physically realizable wheels, frame, and fork that will produce parameter values as close as possible to the target optimal parameter values. We then fabricate and test ride the resulting bicycle.

2 PRESENTED PARAMETER VALUES

We make use of four distinct sets of numerical parameters used with the benchmark bicycle parameterization [2] of the linear Whipple-Carvallo model. We use the same variable names as the benchmark parameterization and thus do not repeat their definitions here.

- **Benchmark values**: Reference values presented in [2] intended to represent typical bicycle with a rigid rider. These values are present simply as a reference due to their ubiquity in characterizing bicycle dynamics.
- **Pista values**: Values estimated from measurements of a Bianchi Pista track style bicycle with a rigid rider from [1].
- **Theoretically optimal values**: Values returned from the optimization procedure described in [3] and herein. These values differ from the Bianchi Pista values in only five of the parameters: wheelbase w, trail c, steer axis tilt λ, front wheel rotational moment of inertia I_{Fyy}, and front wheel radius r_F (see Figure 1).
- **Realized optimal values**: Values derived from a 3D CAD model of a bicycle iteratively designed to have values as close to the "Theoretically optimal values" as possible.

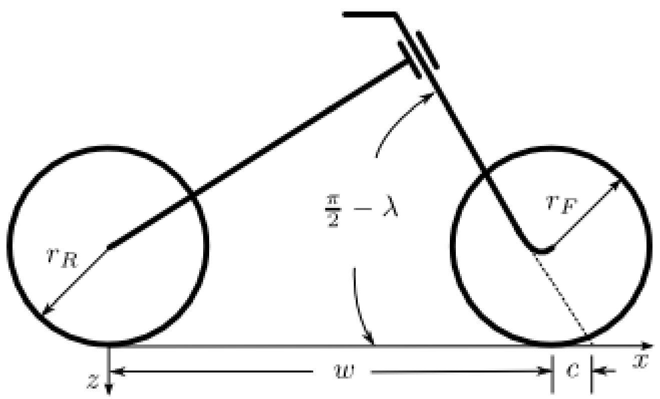

Figure 1. Diagram of the primary geometric parameters of interest.

3 FINDING AN OPTIMAL HANDLING BICYCLE

In the present research, the calculated parameters of an optimally handling bicycle for a 3 m/s forward travel speed were set as the target for practical realization (see Figure 2). This bicycle is identical to the Bianchi Pista with rigid rider presented in [1] except for differing values of the trail, wheelbase, steer axis tilt, front wheel radius, and front wheel inertia about the y-axis.

The optimization procedure used herein is described in [3], except for one modification. With the [3] procedure, it was possible to arrive at front wheel radii that were incompatible with the fixed rotational inertia and mass of the front wheel. We now search for the optimal front wheel rotational inertia, I_{Fyy}, and constrain the front wheel mass or radius to be that which ensures the wheel will have an inertia that is ring-like and thus reasonably realizable.

If the optimizer selects a rotational inertia value larger than that of the initial guess (from the actual Pista wheel) we keep the wheel radius the same as the Pista and add mass such that:

$$m_F = \frac{I_{Fyy}}{r_F^2} \tag{1}$$

If the optimizer selects a rotational inertia value less than the original wheel we keep the mass the same and adjust the radius such that:

$$r_F = \sqrt{\frac{I_{Fyy}}{m_F}} \tag{2}$$

This ensures that we will arrive at a ring-like wheel, which can likely be fabricated. The four free parameters bounds are:

$$-\infty < c < \infty \tag{3}$$

$$\frac{m_H x_H + m_B x_B}{m_H + m_B} < w < \infty \tag{4}$$

$$-\frac{\pi}{2} < \lambda < \frac{\pi}{2} \tag{5}$$

$$\varepsilon < I_{Fyy} < \infty \tag{6}$$

The wheel base bound, Eq. 4, ensures that the bicycle is statically stable in pitch and Eq. 6 prevents division-by-zero resulting from a zero-valued moment of inertia.

We use the CMA-ES derivative-free optimizer [4] as in [3] with the initial standard deviation for each of the four parameters set to $\sigma_c = 0.5\ m$, $\sigma_w = 3\ m$, $\sigma_\lambda = 0.3\pi\ rad$, $\sigma_{I_{Fyy}} = 0.07\ kg\ m$, respectively for each parameter above.

3.1 Target optimal bicycle

Figure 2 shows a pictogram representing the resulting theoretically optimal handling bicycle for a 3 m/s travel speed. The bicycle has a very large positive trail and the wheels overlap. The handlebar/fork rigid body mass center and inertia is the same as the Pista, making it unlikely for a realized fork to match those values due to the span between the steer axis and front wheel. The overlapping wheels are also problematic for steering, but can be remedied by using smaller wheels with equivalent rotational moments of inertia. Lastly, the center of mass of the entire bicycle and rider is only 10 cm left of the front wheel center, making the bicycle relatively easy to tip forward when braking or leaning forward.

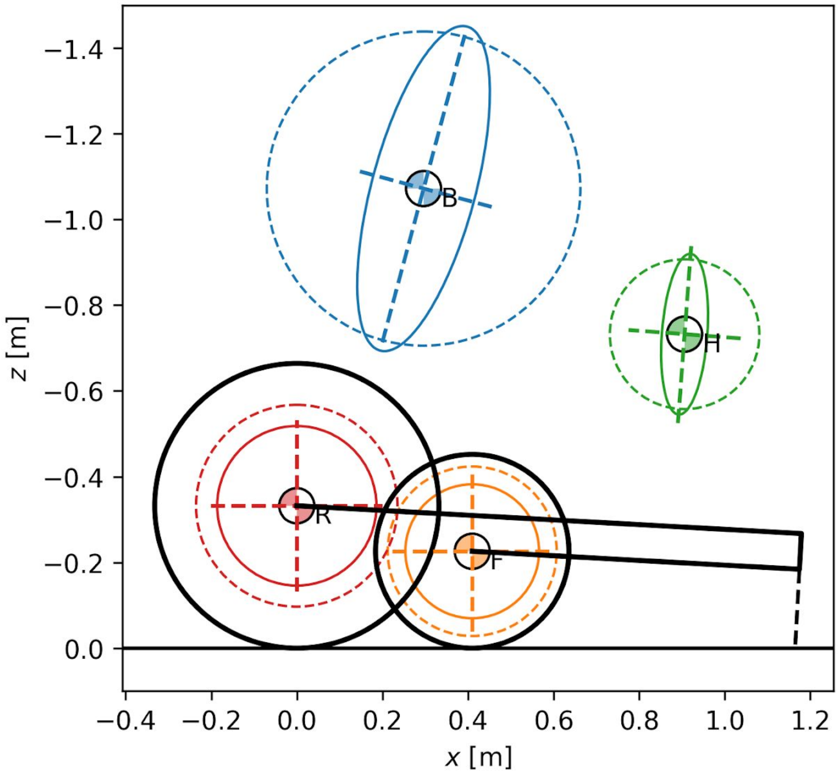

Figure 2. Geometric and inertial depictions of the theoretically optimal values. The following letters represent distinct rigid bodies in this model: R: rear wheel (red), F: front wheel (orange), H: handlebar and fork (green), B: frame and rider (blue). The black lines depict the essential bicycle geometry, the dotted black line is the steer axis, the colored solid lines show the contour of inertially equivalent solid ellipsoids for each rigid body, and the dotted colored lines represent the extents of the central principal radii of gyration of each rigid body.

3.2 The realized bicycle

Starting with the resulting theoretically optimal values as a target, we developed a realistic CAD model that has matching essential geometry and similar inertial values, see Figure 3. The design required many manual iterations to ensure that the realized parameters derived from the CAD model yielded a closed loop stable vehicle and that the HQM remained sufficiently low. If the design produced an unfavorable HQM or was closed loop unstable at any point, it was deemed unacceptable and a new iteration was created. Once the attainable design was fabricated, the CAD model was updated to represent the fabricated product to ensure HQM and closed loop stability were not compromised. Because of the front wheel center being far from the steer axis, the mass and inertia of the front frame assembly must be larger than the target values. We resolved the overlapping wheels by replacing the rear wheel with two stacked smaller wheels that spin in the same direction. The size of each identical smaller wheel was chosen such that the sum of the angular momentum of the two wheels is equivalent to that of the single larger wheel. The roll and yaw moments of inertia of the combined stacked wheels are not equivalent to the single wheel by necessity, but these parameters have significantly less effect on the closed loop stability and HQM than the rotational inertia does. The bicycle is mainly constructed of mild steel round tubing and includes a caster on the front intended to act as a point contact with minimal lateral resistance which keeps the steer axis tilt constant under the weight of the rider.

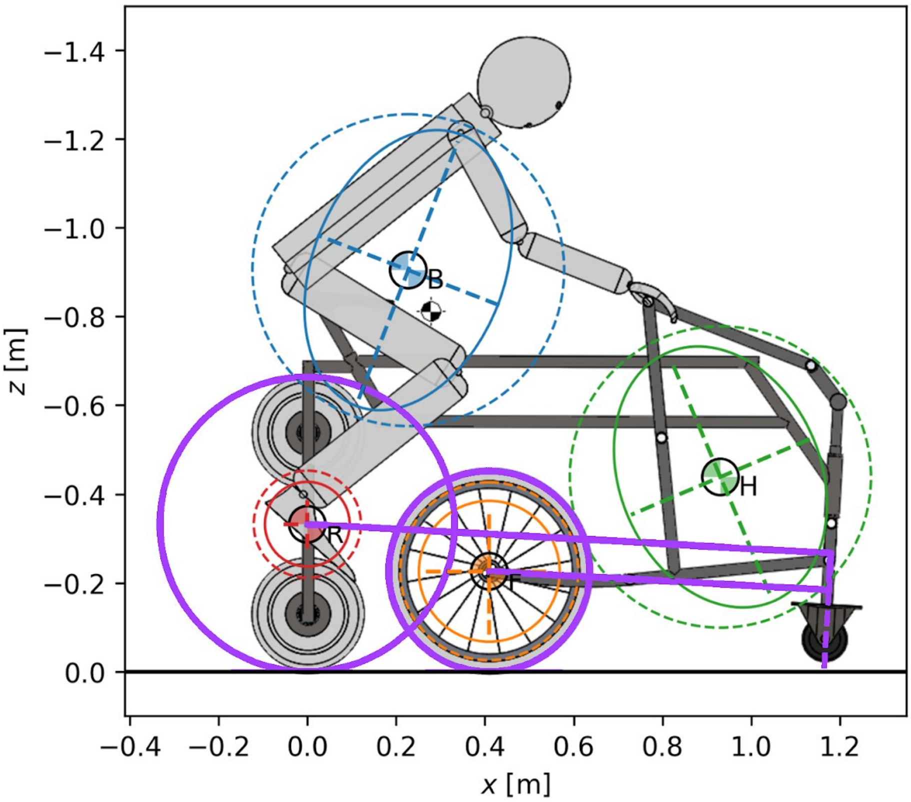

Figure 3. CAD model of the realized bicycle with an overlay of the essential geometry (colored purple) and inertial representations based on the realized optimal values.

4 DYNAMICS AND HANDLING

In order to compare the optimal bicycle design to a conventional design, we present linear analysis and simulation for the benchmark values, Pista values, theoretically optimal values, and realized optimal values. Specifically, we examine the open loop eigenvalues of the Whipple-Carvallo model, examine the closed loop dynamics through the resulting path tracking simulations, and compare the computed HQM for each vehicle.

4.1 Open loop eigenvalues

The open loop eigenvalues give insight into the uncontrolled dynamics of the bicycle-rider system. There is speculation that the open loop eigenvalues correlate to handling in some way, but this has yet to be quantified. Moore et al. show that the idea that open loop stability correlates to handling may have little association [3]. Nevertheless, very large eigenmode time constants are likely to be hard to control. Frequency modes outside of or aligned with the human's neuromuscular bandwidth may also cause handling difficulties. Table 1 provides the eigenvalues of the four bicycles at a 3 m/s travel speed. All four parameter sets exhibit the classically defined weave mode. The benchmark and Pista exhibit a stable capsize mode and very stable caster mode, as expected from typical bicycles. The optimal bicycles have almost double the weave frequency, a slightly stable caster mode, and an unstable capsize mode. The typical bicycles (Benchmark and Pista) are unstable due their weave mode at 3 m/s, while the optimal bicycles have stable weave modes at this travel speed. Conversely the capsize mode is unstable for the optimal handling bicycles, but the time constants are reasonable for human control.

Table 1. Values of the open loop eigenvalues for the four bicycles at 3 m/s.

Eigenmode	Benchmark	Pista	Theoretical Optimal	Realized Optimal
Weave	1.7068 +/- 2.3158i	1.5142 +/- 1.6953i	-2.8327 +/- 3.1209i	-2.3999 +/- 1.7761i
Capsize	-2.6337	-3.0317	2.1177	2.5144
Caster	-10.351	-12.3648	-2.9410	-3.5143

The eigenvalues of the realized bicycle can be examined over a range of speeds for general comparisons to more typical bicycles. Figure 4 shows the eigenvalue parts as a function of travel speed. There is a stable roll-steer oscillatory eigenmode that becomes non-oscillatory around 6 m/s, opposite in nature to a typical bicycle with respect to speed. There is also a stable real mode and an unstable real mode up to 10 m/s. This bicycle is interestingly unstable for a typical range of riding speeds, including the target design speed of 3 m/s.

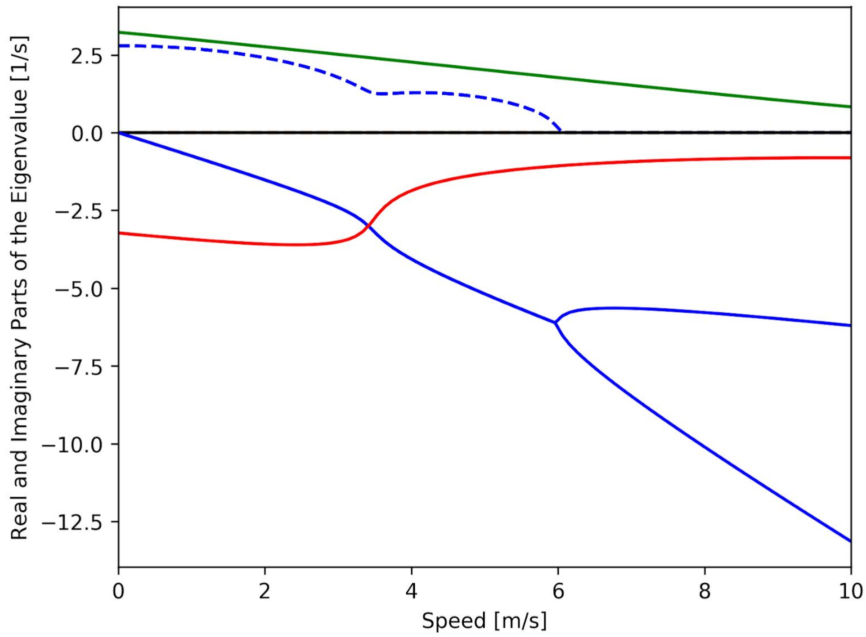

Figure 4. Real (solid) and imaginary (dashed) parts of the open loop eigenvalues of the realized bicycle. The colors represent the different eigenmodes of the fourth order system.

4.2 Closed Loop Dynamics

Using the controller defined in [1] and the updated gain selection technique described in [5], human-like bandwidth-limited control is implemented for evaluating path tracking simulations. Table 2 provides the five controller gains required to close the feedback loops for each of the parameter value sets.

Table 2. Controller gains found for all four bicycle designs at 3m/s.

Gain	Benchmark	Pista	Theoretically Optimal	Realized Optimal
k_{δ}	27.9091	27.9233	0.0165	0.0089
$k_{\dot{\varphi}}$	-0.0924	-0.1152	-3499.4479	-8897.1495
k_{φ}	15.3676	13.2661	4.5382	2.6857
k_{ψ}	0.0871	0.0834	0.1039	0.1
k_{y_q}	0.1557	0.1684	0.1416	0.1414

Figure 4 shows a 2-meter lane change at a 3 m/s travel speed. All bicycles perform the maneuver stably with good performance. The benchmark and Pista bicycles have similar performance. The theoretical optimal and realized optimal bicycles have almost identical performance, but have a closed loop mode that is less damped than the more typical bicycles. Nevertheless, all the bicycles make the lane change at a similar performance level as expected using the controller gain selection method. The fact that the realized optimal has also identical closed loop dynamics as the target theoretical optimal even with parameters values that are not identical, gives credence to our realized design and its predicted optimal handling.

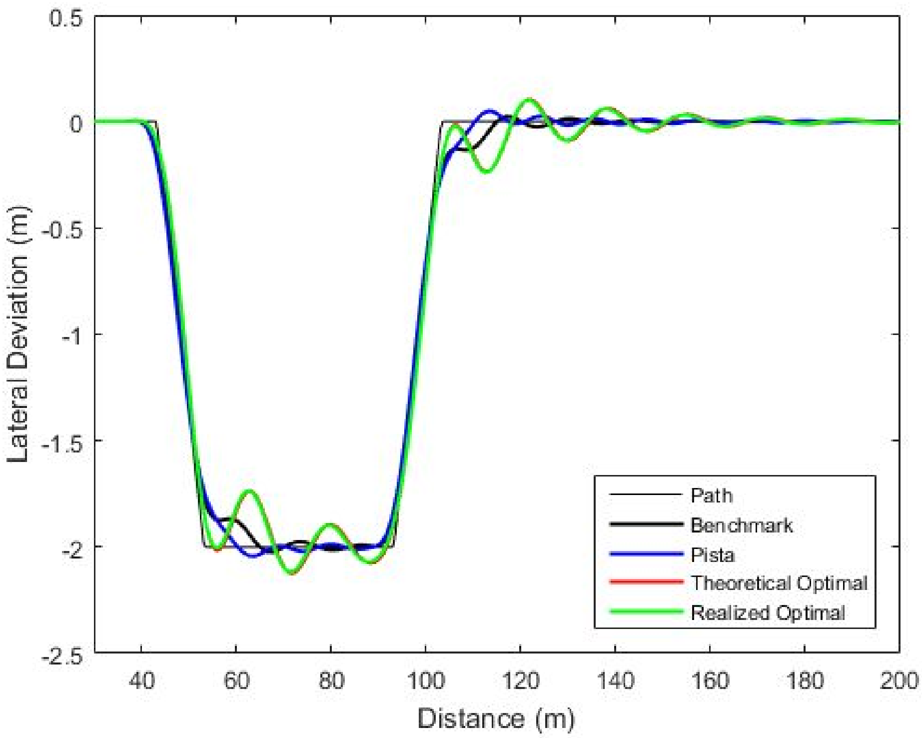

Figure 4. Simulation of the four bicycles performing a 2-meter lane change maneuver at 3 m/s. Curves indicate the path of the front wheel contact point on the ground plane.

4.3 Handling Quality Metric

Once the control gains are determined, the theoretical HQM derived in [1] can be computed. Figure 5 shows the HQM as a function of frequency for four bicycle designs (which all include a rigid rider). The peak values are summarized in Table 3 and show that we obtain a threefold improvement in handling with the realized optimal as compared to the Pista. This is an equivalent improvement in handling as one gets at riding the Pista at 7.5 m/s versus 2.5 m/s [1]. It is also worth noting that the benchmark values are predicted to have very poor handling at 3 m/s, indicating that the values may not reflect a typical bicycle as the HQM peak is usually between 9 and 16 for typical bicycles at that speed [1].

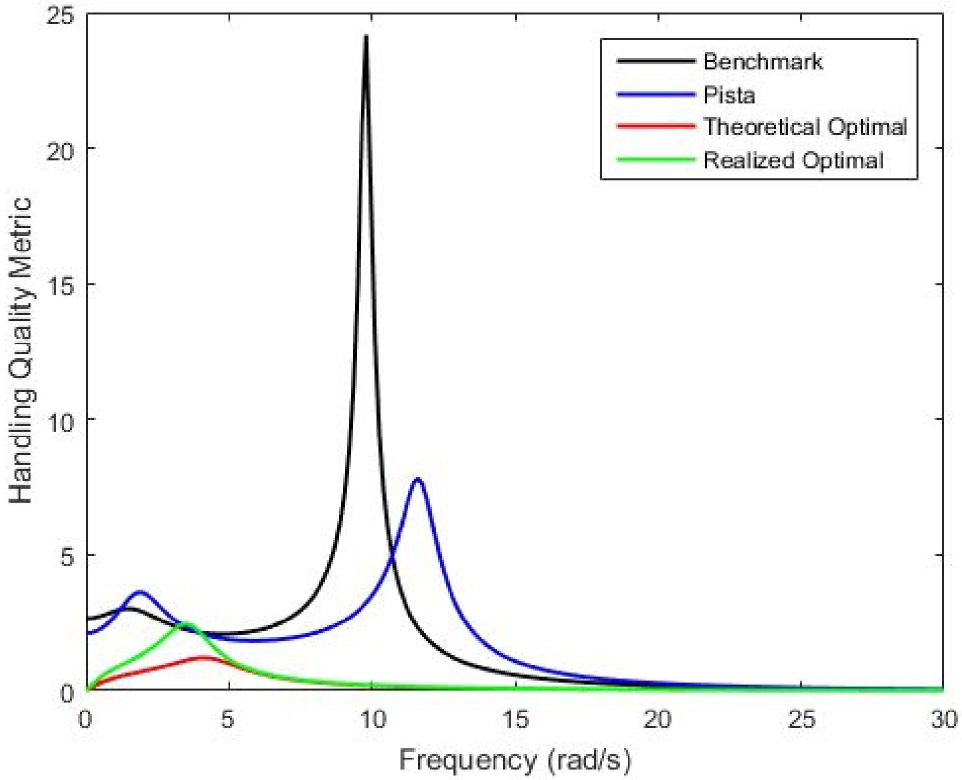

Figure 5: HQM vs. frequency for the benchmark, pista bicycle, theoretical optimal, and realized optimal values at a travel speed of 3 m/s.

Table 3. Peak HQM Values:

Benchmark	Pista	Theoretical Optimal	Realized Optimal
22.94	7.79	1.20	2.45

5 FABRICATED BICYCLE

After verifying that the predicted dynamics and HQM were optimal for the realized optimal values, we fabricated the bicycle from off-the-shelf parts and mild steel tubing (Figure 6). When comparing the fundamental geometries of the target modeled bicycle to the fabricated bicycle, the wheelbase was smaller than the target by 0.04 m, the trail was larger than the target by 0.003 m, the front wheel radius was smaller by 0.004 m, and the steer axis tilt should remain near the target -3.14° with the addition of the caster wheel compensating for deflections. The fabricated bicycle uses a small bicycle wheel for the front wheel and two identical cart wheels for the rear set. The rear set has fixed cogs on the hubs connected via a bicycle chain so the wheels spin at the same angular rate. The front end of the bicycle was especially difficult to design due to the large trail and the necessity to provide handholds for the rider. The front frame is very susceptible to large deflections under the rider's weight and currently requires a swiveling caster to support the front of the frame under the steer tube. The caster acts as a frictionless spacer between the ground and the frame. With the addition of the caster, the bicycle is rideable. However, due to the lack of pedals, the bicycle requires propulsion from either a second party pushing the rider or a running start. At the time of writing, we have attempted straight-line riding on smooth, flat ground. The large positive trail requires a shift in the rider's steering intuition to focus on using the steer to effectively roll the frame and point the head tube in the desired direction of travel. It does not feel as "nimble" as the track bicycle it was based on, but a track bicycle is anecdotally considered to require more close attention when maneuvering. Our bicycle, on the other hand, is more reminiscent of a beach cruiser bicycle used mostly for "relaxed" riding.

Figure 6. Fabricated bicycle with and without a rider seated in the optimal position. The front end in supported by a stack of books in the left photo, but this is replaced with a swiveling caster when riding.

6 DISCUSSION AND CONCLUSIONS

In the course of the present research, we found that designing a bicycle which realizes theoretically optimal parameters results in a highly unconventional arrangement. The vehicle designed is based on an existing conventional bicycle, but ultimately had several features that did not conform to a more standard bicycle frame design. We were able to successfully fabricate a bicycle that has almost identical open and closed loop dynamics as the theoretical optimal target design. This is difficult due to the fact that we optimized mostly the geometric parameters and left the inertial parameters the same as the track bicycle. This creates a design conundrum since the inertial aspects are strict functions of the underlying geometry. Our design's large positive trail, dual rear wheels, and extremely short wheelbase are completely unorthodox but shown to perform and handle well in our simulations. Despite this unorthodox design, our realized optimal design has a computed HQM less than a third that of the Bianchi Pista bicycle it is based on. This improvement in handling is akin to the improvement in handling gained by increasing the bicycle's travel speed, but accomplished by manipulating the geometry instead.

Additionally, we found that although it is possible to design a bicycle that realizes optimal geometric, mass, and inertial parameters, doing so does not always coincide with creating a structure with sufficient strength and stiffness. Arriving at a design that is both rideable and approximates the optimal parameters requires repeated iteration and often precludes realizing the optimal parameters exactly. Advanced optimization methods could attempt to balance both structural integrity and optimal handling characteristics to produce parameter sets that are more straightforward to design, fabricate, and test. Dynamic testing of the fabricated bicycle remains to be done in order to validate the real-world performance of this design against its simulated performance and is left for future work.

REFERENCES

[1] R. Hess, J. K. Moore, and M. Hubbard, "Modeling the Manually Controlled Bicycle," IEEE Transactions on Systems, Man, and Cybernetics - Part A: Systems and Humans, vol. 42, no. 3, pp. 545–557, Feb. 2012.

[2] J. P. Meijaard, J. M. Papadopoulos, A. Ruina, and A. L. Schwab, "Linearized dynamics equations for the balance and steer of a bicycle: A benchmark and review," Proceedings of the Royal Society A: Mathematical, Physical and Engineering Sciences, vol. 463, no. 2084, pp. 1955–1982, Aug. 2007.

[3] J. Moore, M. Hubbard, and R. A. Hess, "An Optimal Handling Bicycle," in Proceedings of the 2016 Bicycle and Motorcycle Dynamics Conference, 2016.

[4] Hansen and Ostermeier, "Adapting arbitrary normal mutation distributions in evolution strategies: The covariance matrix adaptation," in *Proceedings of the 1996 IEEE International Conference on Evolutionary Computation*, 1996, pp. 312–317.

[5] J. K. Moore, "Human Control of a Bicycle," Doctor of Philosophy, University of California, Davis, CA, 2012.

APPENDIX

Table 4. Theoretically Optimal and Realized Optimal Parameter Values

Parameter	**Theoretically Optimal**	**Realized Optimal**
w (m)	0.35996	0.41
c (m)	0.75461	0.74561
λ (rad)	-0.05486	-0.05486
g (N-kg^{-1})	9.81	9.81
r_R (m)	0.3321	0.332
m_R (kg)	1.38	5.349
I_{Rxx} (kg-m^2)	0.05535	0.0157
I_{Ryy} (kg-m^2)	0.07641	0.078
x_B (m)	0.2963	0.2275
z_B (m)	-1.072	-0.9044
m_B (kg)	76.49	65.48
I_{Bxx} (kg-m^2)	9.978	5.926
I_{Bxz} (kg-m^2)	-2.123	-1.062
I_{Byy} (kg-m^2)	10.27	8.077
I_{Bzz} (kg-m^2)	2.648	3.578
x_H (m)	0.9063	0.9309
z_H (m)	-0.7324	-0.4385
m_H (kg)	2.27	6.729
I_{Hxx} (kg-m^2)	0.09799	0.511
I_{Hxz} (kg-m^2)	-0.004408	0.0799
I_{Hyy} (kg-m^2)	0.06925	0.775
I_{Hzz} (kg-m^2)	0.03961	0.3559
r_F (m)	0.226	0.226
m_F (kg)	1.58	1.548
I_{Fxx} (kg-m^2)	0.05523	0.0314
I_{Fyy} (kg-m^2)	0.1062	0.0623